

Supporting Information for

**Affinity-Driven Design of Cargo-Switching
Nanoparticles to Leverage a Cholesterol-Rich
Microenvironment for Atherosclerosis Therapy**

Heegon Kim^{1,2}, Sandeep Kumar³, Dong-Won Kang³, Hanjoong Jo^{3,4}, and Ji-Ho Park^{1,2,}*

¹Department of Bio and Brain Engineering, and ²KAIST Institute for Health Science and Technology, Korea Advanced Institute of Science and Technology (KAIST), Daejeon, 34141, Republic of Korea, ³Wallace H. Coulter Department of Biomedical Engineering, Georgia Institute of Technology and Emory University, and ⁴Division of Cardiology, Department of Medicine, Emory University, Atlanta, GA 30322, USA

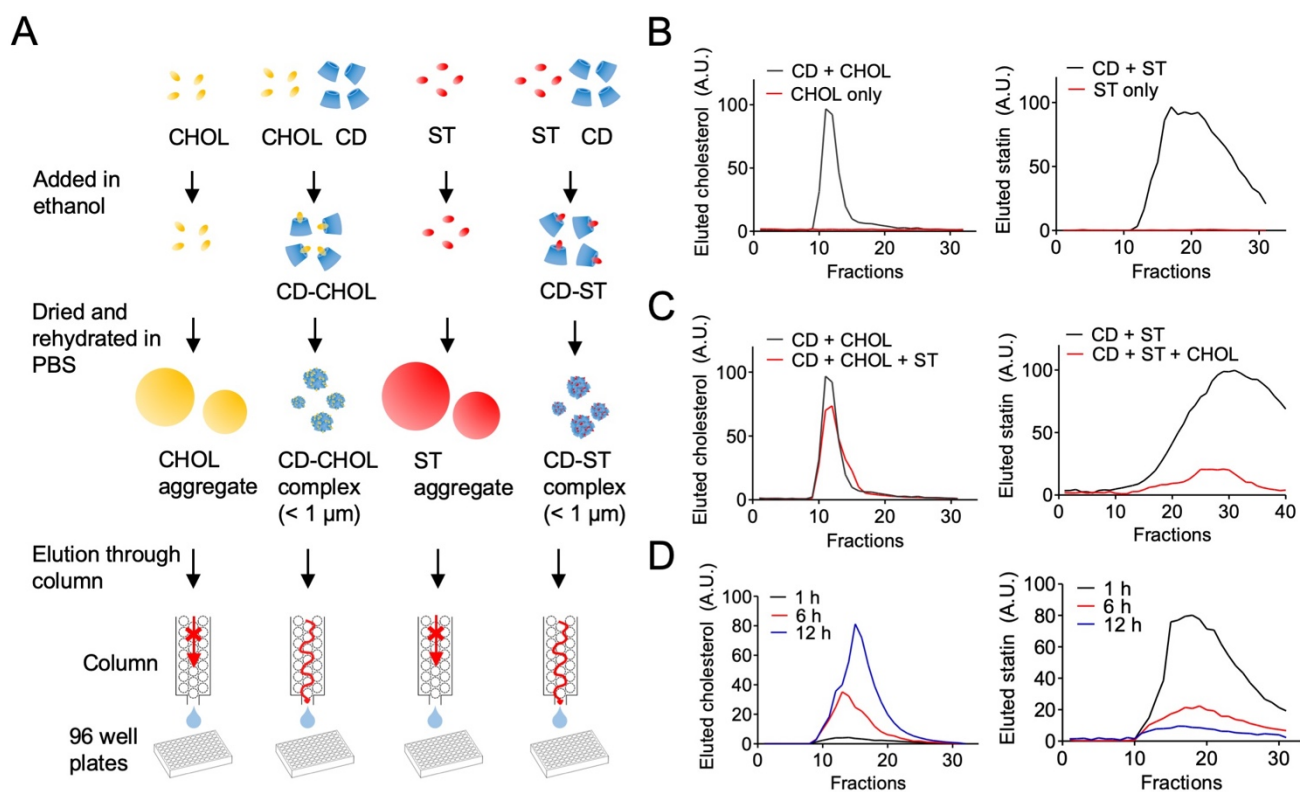


Figure S1. Competitive binding and cargo-switching assay using size exclusion chromatography. (A) Schematic of size exclusion chromatography. While hydrophobic molecules such as cholesterol (CHOL) and statin (ST) cannot be eluted through the column due to excessive aggregation, their interaction with cyclodextrin (CD) and formation of nanocomplexes allows the elution of CHOL and ST in the form of CD-CHOL and CD-ST complexes. (B) Formation and size exclusion chromatography of CHOL-CD or ST-CD nanocomplexes. The solution containing CHOL (5 mM, contains 2 % NBD-CHOL), ST (5 mM), CHOL (5 mM, contains 2 % NBD-CHOL) + CD (30 mM), or ST (5 mM) + CD (30 mM) was eluted using a PD-10 column. Nanocomplexation with CD allows elution of CHOL and ST through the column. Representative elution profiles of CHOL either with or without CD (left) and those of ST either with or without CD. Results are representative of three independent experiments (right). (C) Competitive binding assay. The solution containing CHOL (5 mM, contains 2 % NBD-CHOL), ST (5 mM), or CD (30 mM) was mixed in ethanol, dried, and then rehydrated in PBS. The solution was then eluted using a PD-10 column and the fractions were collected in a 96-well plate. Representative elution profiles of CHOL (left) and ST (right) are shown. (D) Cargo-switching assay. CHOL (5 mM, contains 2 % NBD-CHOL) was added to the solution containing CD-ST nanocomplexes (30 mM CD and 5 mM ST). The solution was eluted through a PD-10 column at 1, 6, and 12 hours after incubation. Representative elution profiles of CHOL (left) and ST (right) after different incubation times were shown. Results are representative of three independent experiments. Quantification of CHOL and ST was performed by measuring fluorescence of NBD-CHOL (excitation: 480 nm/emission: 530 nm) and absorbance of ST (at 240 nm).

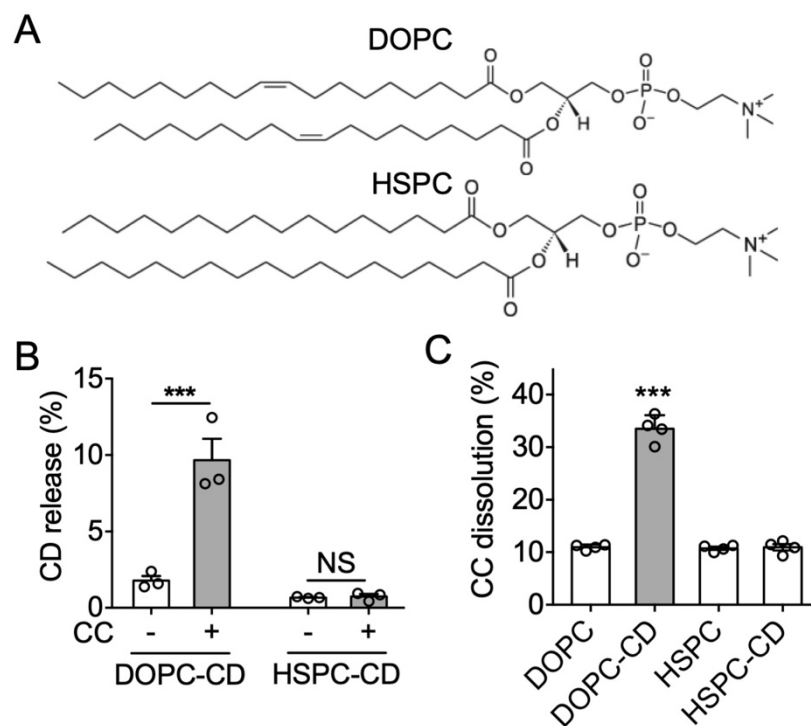


Figure S2. CC-mediated disruption of DOPC-based liposomal membrane at 37 °C. (A) Chemical structures of DOPC and HSPC. (B) Percentage of CD release from liposomal CD after incubation with or without CC for 24 hours. DOPC liposomes encapsulated with RBITC-labeled CD (DOPC-CD) or HSPC liposomes encapsulated with RBITC-labeled CD (HSPC-CD) were incubated either with or without CC for 24 hours at 37 °C and then collected to quantify the percentage of released CD. (C) CC dissolution with liposomes and liposomal CD. NBD-labeled CC were incubated with DOPC-based liposomes (DOPC), DOPC-CD, HSPC-based liposomes (HSPC), or HSPC-CD for 24 hours at 37°C and then filtered out to quantify the percentage of dissolved cholesterol. Data are mean ± s.e.m. [NS, not significant; n = 3, ***P < 0.001, unpaired two-tailed Student's t test for (B); n = 4, ***P < 0.001 versus all other groups, unpaired two-tailed Student's t test for (C)].

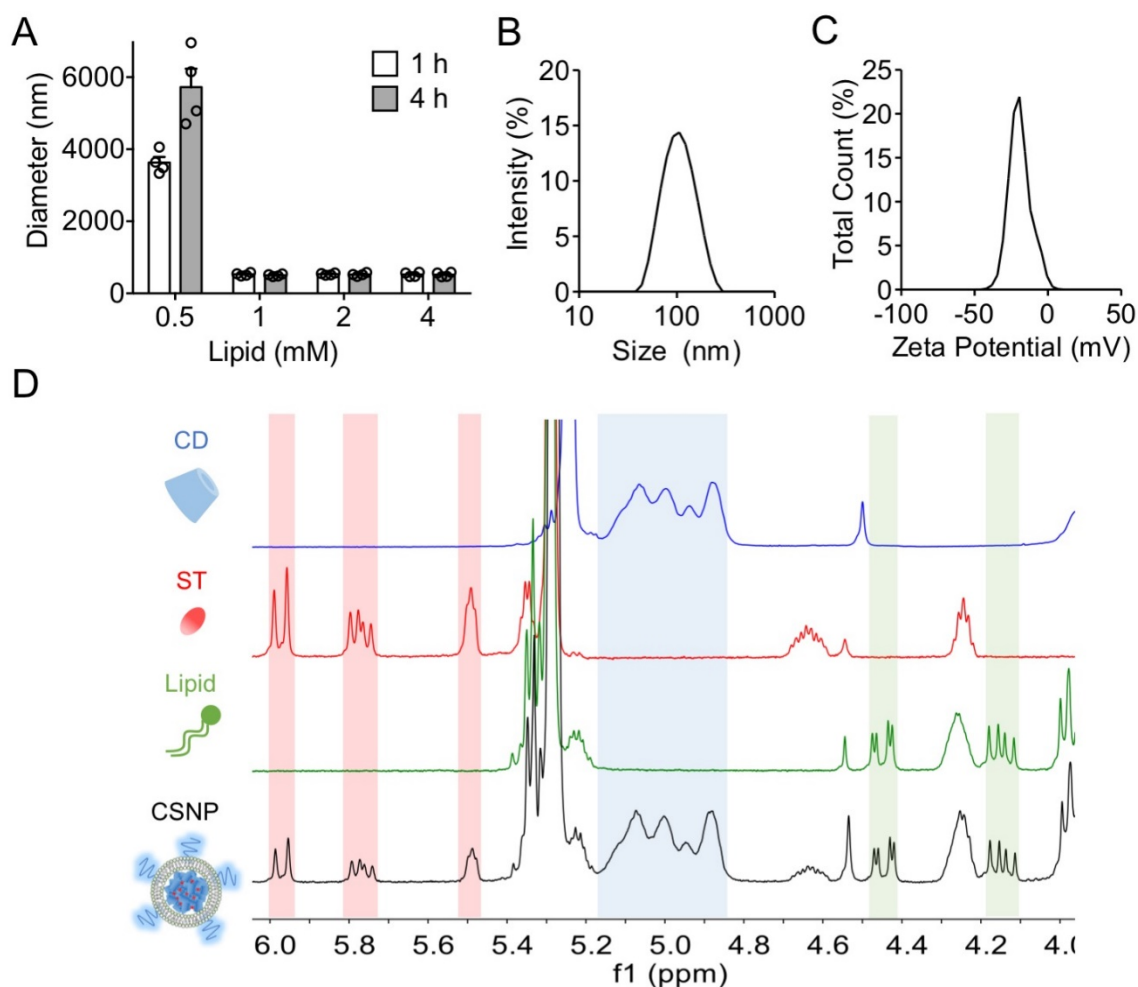


Figure S3. Preparation and physicochemical properties of CSNP. (A) Optimization of total lipid concentration to coat the CSNP. The lipid film prepared at different total concentrations of lipids was hydrated with the solution containing CD-ST complexes with 1 mM ST and 6 mM CD. The resulting lipid-coated complexes were incubated in PBS for 1 and 4 hours and the hydrodynamic size at each time was measured by dynamic light scattering. We chose 1 mM lipids to prepare the CD-ST nanocomplexes because this lipid concentration allowed stabilization of the complex with minimum amount of lipids. (B) Distribution of hydrodynamic sizes of CSNP measured by dynamic light scattering. (C) Distribution of zeta potentials of CSNP measured by dynamic light scattering. (D) Representative 1H-NMR spectrum of CD (blue), ST (red), LP (green), and CSNP (black) dissolved in ethanol-d₆ with 1% TMS. Data are means \pm s.e.m. (n=4).

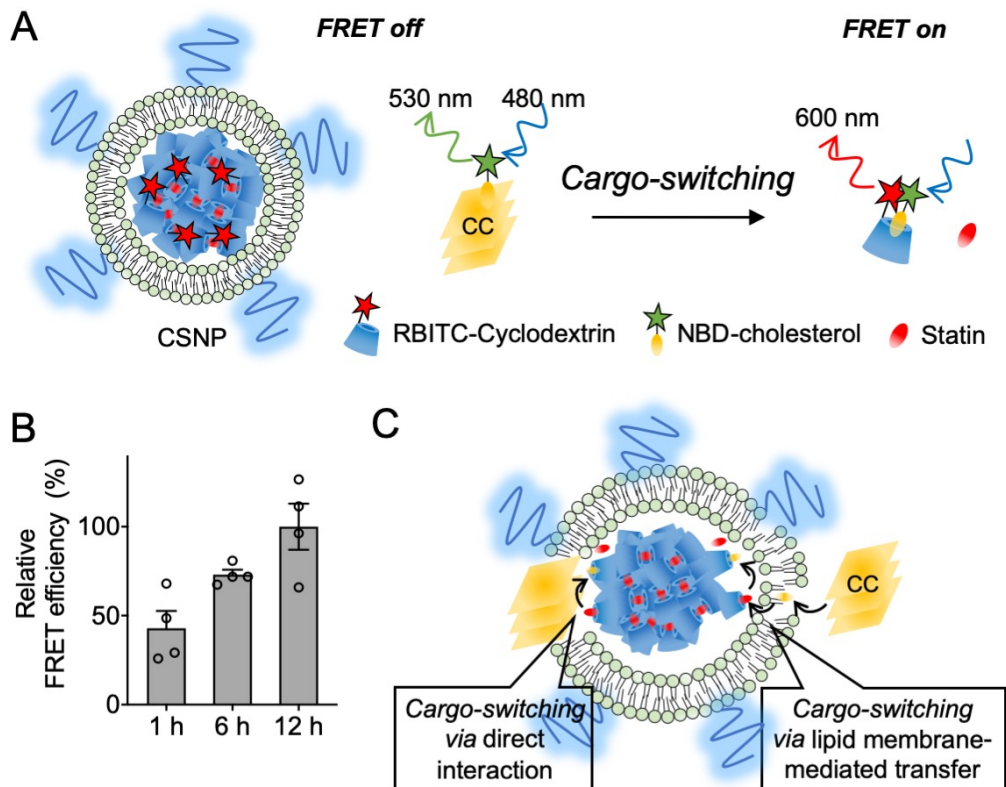


Figure S4. FRET assay for demonstration of cargo-switching. (A) Schematic of FRET between RBITC-cyclodextrin and NBD-cholesterol *via* cargo-switching. (B) Relative FRET efficiency at 1, 6, and 12 h after incubation of CSNP with cholesterol crystal (CC). (C) Schematic of cargo-switching mechanism of CSNP upon interaction with CC. The inner CD-ST complex interacts with CC either directly through the disrupted membrane or indirectly *via* the lipid membrane. The results are representative of three independent experiments. Data are means \pm s.e.m. ($n = 4$).

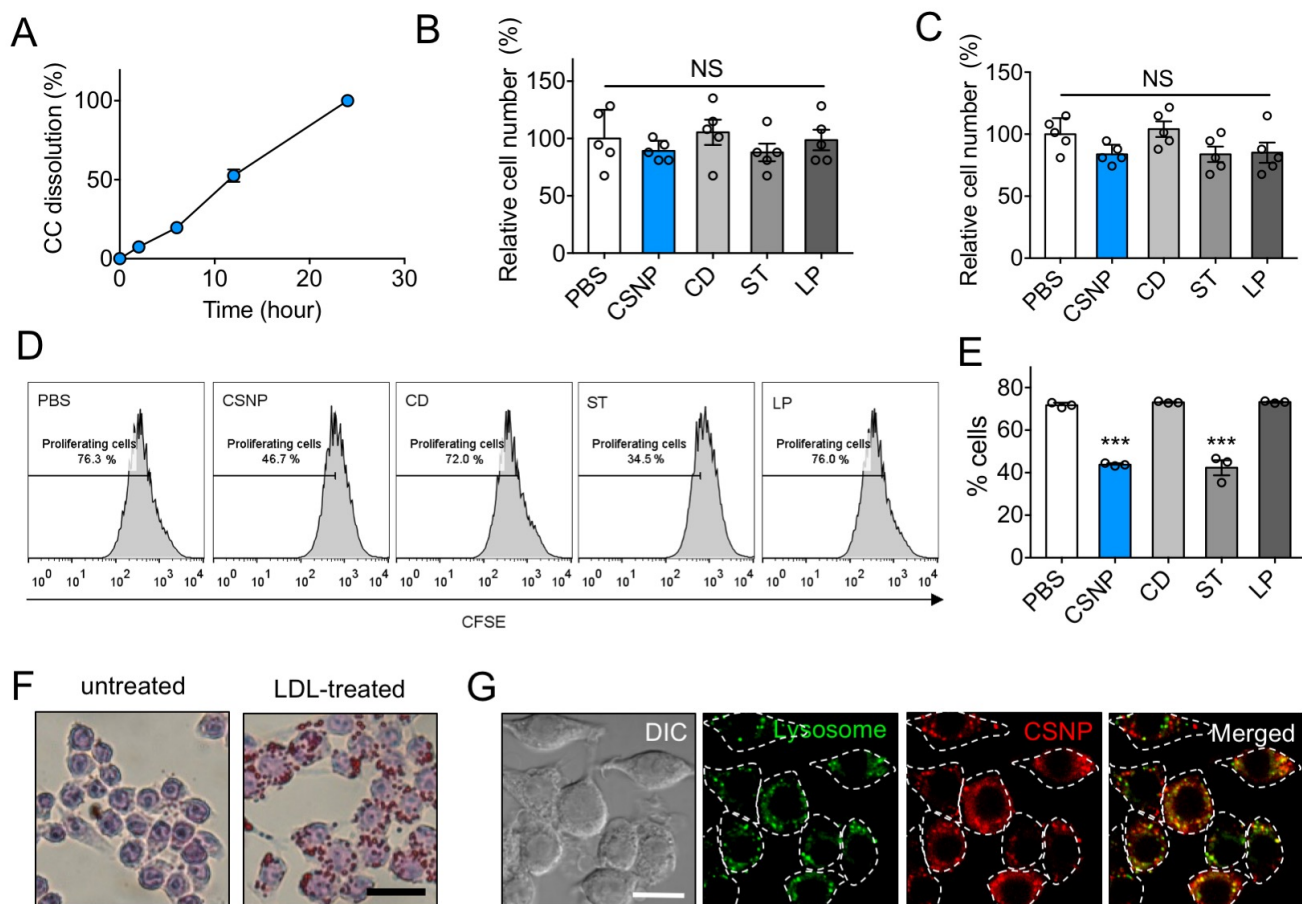


Figure S5. Anti-atherogenic effects of CSNP *in vitro*. (A) Time dependent CC dissolution with CSNP. (B and C) Relative cell number of macrophages. Cells were treated with lipopolysaccharide (LPS) for 24 hours (B) or LPS and CC for 24 hours (C), respectively. The cells were then treated with CSNP for 48 hours at a statin concentration of 5 μ M and the cell number was counted. (D) Anti-proliferative effects of CSNP on macrophages. Raw 264.7 cells were labelled with Celltrace™ CFSE reagents and treated with various samples for 48 hours. The percentage of proliferating cells of the total treated cells was determined using flow cytometry. Results are representative of two independent experiments. (E) Quantification of proliferating cells in (D). (F) Representative bright field microscopic images of untreated and LDL-treated macrophages. Raw 264.7 cells were treated with LDL for 24 hours and stained with Oil-Red-O and hematoxylin. Scale bar indicates 20 μ m. (G) Representative confocal microscopic images of macrophages taking up CSNP. Lysosomes were stained with LysoTracker (green). The dotted circles indicate individual cells. The scale bar indicates 10 μ m. Data are means \pm s.e.m. [n = 4 for (A); n = 5 for (B) and (C); n = 3 for (E); NS, not significant; one-way ANOVA and Tukey's multiple comparisons test for (B) and (C); ***P < 0.001, unpaired two-tailed Student's t test compared to PBS for (E)].

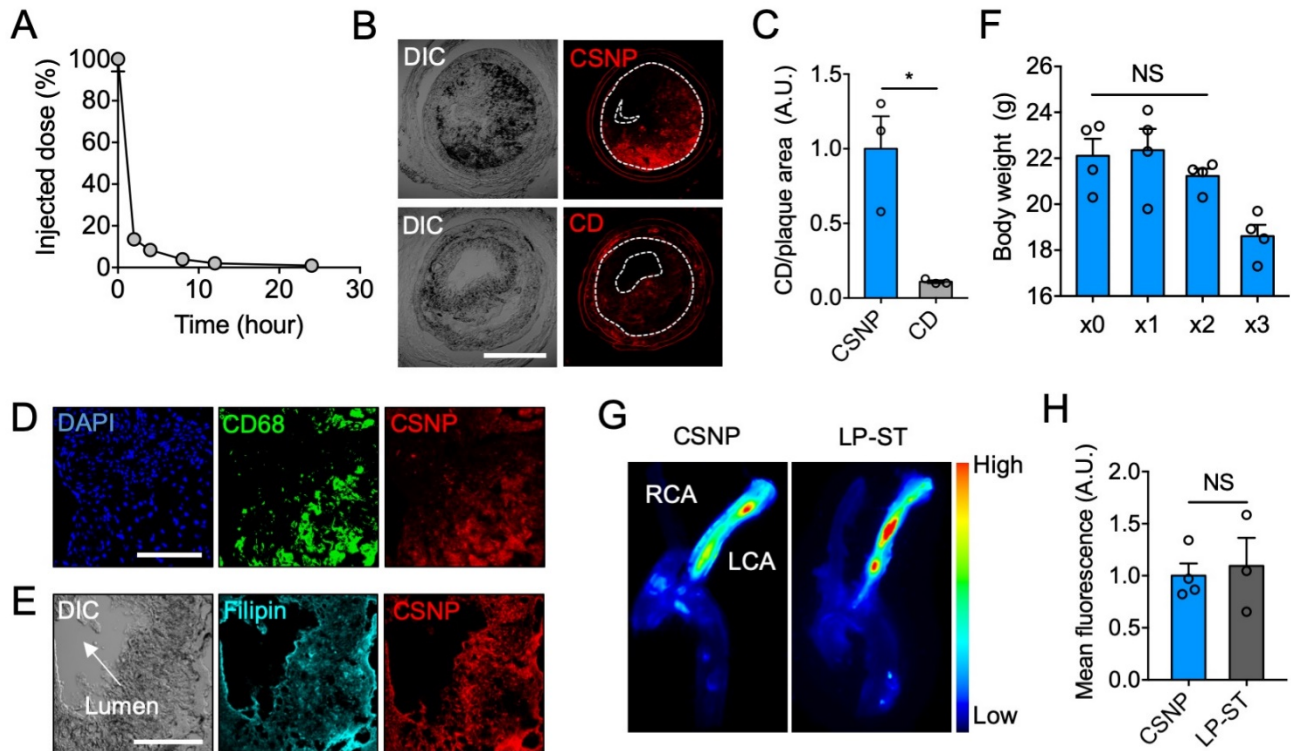


Figure S6. Pharmacokinetics and plaque targeting of CSNP, cyclodextrin and liposomal statin. (A) Pharmacokinetics of cyclodextrin. (B) Representative fluorescence images of the LCA sections showing accumulation of CSNP (top) and cyclodextrin (CD, bottom) in the plaques. The dotted lines indicate plaque area. The scale bar indicates 200 μm . (C) Quantification of the fluorescence in (B). (D and E) Representative confocal fluorescence images of the LCA sections after staining macrophages (D) and cholesterol (E). Anti-CD68 antibody and Hoechst were used to stain macrophage (green) and nucleus (blue), respectively. Filipin was used to stain cholesterol (cyan). The scale bars indicate 100 μm . (F) Body weight of ApoE^{-/-} mice on day 2 after intravenous injection of CSNP at various doses. CSNP (100 mg/kg cyclodextrin and 15 mg/kg statin) were concentrated 2-fold (x2) and 3-fold (x3) in PBS. (G) Representative *ex vivo* fluorescence images of the dissected carotid arteries showing accumulation of CSNP (left) and liposomal statin (LP-ST, right). (H) Quantification of the fluorescence in (G). Data are means \pm s.e.m. [n = 3 for (A) and (C); n = 4 for (F) and (H); NS, not significant; *P < 0.05, unpaired two-tailed Student's t test, compared to x0 for (F)].

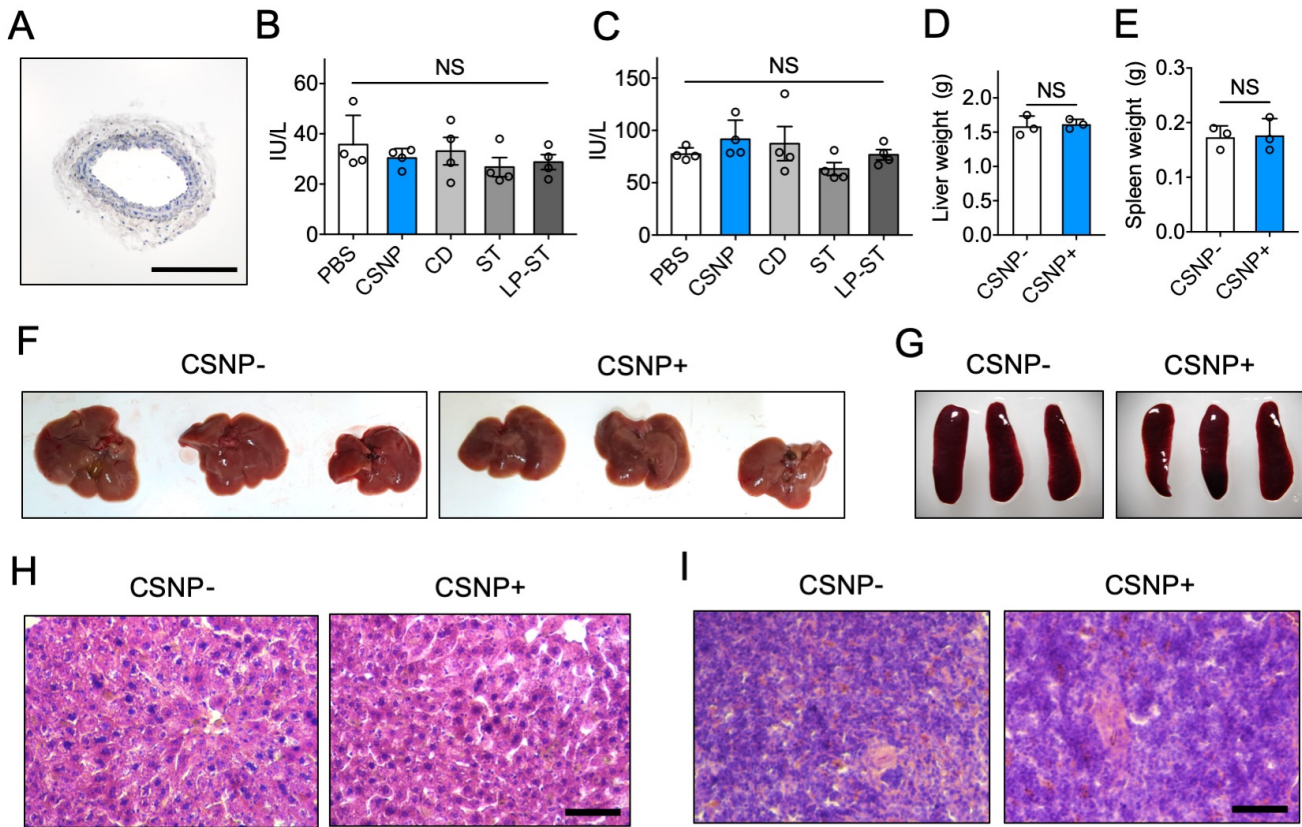


Figure S7. Liver and spleen toxicity of CSNP after anti-atherogenesis therapy. (A) Representative histological image of the non-ligated LCA section after Oil-Red-O staining. The scale bar indicates 200 μ m. (B and C) Liver toxicity examined by measuring alanine transaminase (ALT) (B) and aspartate transaminase (AST) (C) in bloods. (D and E) Weight of liver (D) and spleen (E). (F and G) Bright field images of liver (F) and spleen (G). (H and I) Representative H&E staining images of liver (H) and spleen (I). The scale bars indicate 100 μ m. CSNP+ and CSNP- indicate intravenous injection of CSNP and PBS, respectively. Data are means \pm s.e.m. [n = 4 for (B) and (C); n = 3 for (D) and (E); NS, not significant; one-way ANOVA and Tukey's multiple comparisons test for (B) and (C); unpaired two-tailed Student's t test for (D) and (E)].

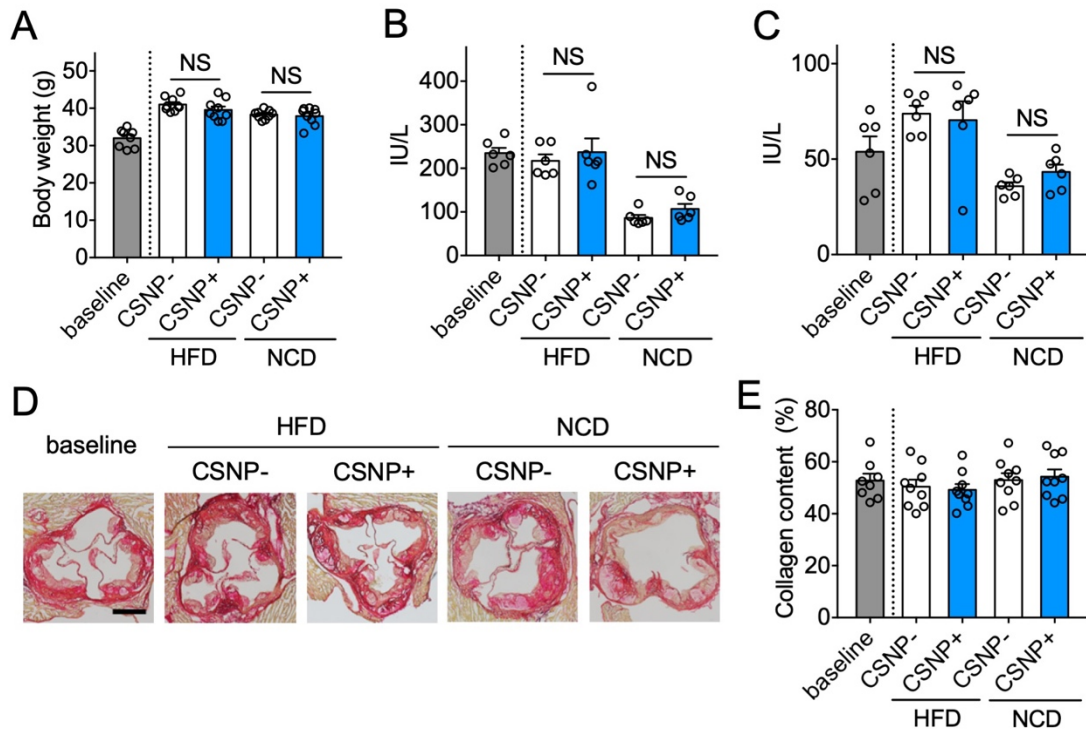


Figure S8. Assessment of systemic side effects and plaque vulnerability after CSNP treatment. (A) Mouse body weight change during treatment. Mice fed with HFD for 12 weeks (baseline) were injected intravenously with PBS (CSNP-) or CSNP (CSNP+) twice a week for 4 weeks and the diet was either maintained (HFD group) or switched to a normal chow-diet (NCD group). (B and C) Liver toxicity examined by measuring alanine transaminase (ALT). (B) and aspartate transaminase (AST) (C) in bloods. (D) Representative histological images of aortic root sections after picrosirius red staining. (E) Quantification of collagen content in the aortic root sections after antiatherogenic therapy in (D). CSNP+ and CSNP- indicate intravenous injection of CSNP and PBS, respectively. Scale bar indicates 200 μ m. Data are means \pm s.e.m. [n = 8 (baseline group) or 9 (other groups) for (A) and (E); n=6 for (B) and (C); NS, not significant; unpaired two-tailed student's t-test].

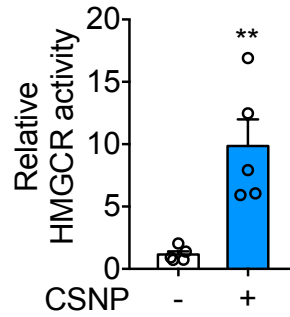


Figure S9. Change of HMG-CoA reductase (HMGCR) activity after CSNP treatment in wild-type mice. Mice were injected intravenously with PBS (CSNP-) or CSNP every 3 days (total of four times). Three days after last injection, livers were harvested and the HMG-CoA reductase activity was measured. CSNP+ and CSNP- indicate intravenous injection of CSNP and PBS, respectively. Data are means \pm s.e.m. (n = 5; **P < 0.01, unpaired two-tailed Student's *t* test).